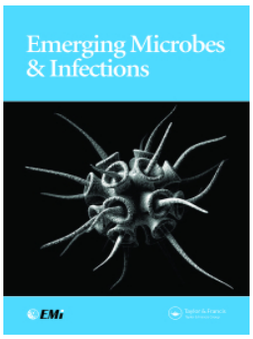

Emerging Microbes & Infections

ISSN: 2222-1751 (Online) Journal homepage: www.tandfonline.com/journals/temi20

Genetic characterization of influenza A viruses circulating in Hong Kong, China, 2023: the first influenza epidemic after the lifting of 2.5 years of COVID-19 non-pharmaceutical interventions

Jingyuan Bian, Joshua Fung, Lam-Kwong Lee, Wing-Yin Tam, Leo Chun-Hei Wong, Cyrus Ka-Wo Wong, Maverick Yu-Xuan Lau, Bei Jiang, Nicky Ho-Laam Tang, Alex Yat-Man Ho, Miranda Chong-Yee Yau, Jason Chi-Ka Cheng, Kristine Shik Luk, May Kin-Ping Lee, Jimmy Yiu-Wing Lam, Sandy Ka-Yee Chau, Qing Xiong, Gilman Kit-Hang Siu & Franklin Wang-Ngai Chow

To cite this article: Jingyuan Bian, Joshua Fung, Lam-Kwong Lee, Wing-Yin Tam, Leo Chun-Hei Wong, Cyrus Ka-Wo Wong, Maverick Yu-Xuan Lau, Bei Jiang, Nicky Ho-Laam Tang, Alex Yat-Man Ho, Miranda Chong-Yee Yau, Jason Chi-Ka Cheng, Kristine Shik Luk, May Kin-Ping Lee, Jimmy Yiu-Wing Lam, Sandy Ka-Yee Chau, Qing Xiong, Gilman Kit-Hang Siu & Franklin Wang-Ngai Chow (2025) Genetic characterization of influenza A viruses circulating in Hong Kong, China, 2023: the first influenza epidemic after the lifting of 2.5 years of COVID-19 non-pharmaceutical interventions, Emerging Microbes & Infections, 14:1, 2521850, DOI: 10.1080/22221751.2025.2521850

To link to this article: https://doi.org/10.1080/22221751.2025.2521850

Emerging Microbes & Infections
2025, VOL. 14, 2521850 (15 pages)
https://doi.org/10.1080/22221751.2025.2521850

Genetic characterization of influenza A viruses circulating in Hong Kong, China, 2023: the first influenza epidemic after the lifting of 2.5 years of COVID-19 non-pharmaceutical interventions

Jingyuan Bian [a]*, Joshua Fung [a]*, Lam-Kwong Lee[a]*, Wing-Yin Tam[a], Leo Chun-Hei Wong[a], Cyrus Ka-Wo Wong [a], Maverick Yu-Xuan Lau[a], Bei Jiang [a], Nicky Ho-Laam Tang[a], Alex Yat-Man Ho[b], Miranda Chong-Yee Yau [c], Jason Chi-Ka Cheng[d], Kristine Shik Luk[b], May Kin-Ping Lee[b], Jimmy Yiu-Wing Lam[c], Sandy Ka-Yee Chau[d], Qing Xiong [a], Gilman Kit-Hang Siu [a] and Franklin Wang-Ngai Chow [a]

[a]Department of Health Technology and Informatics, Faculty of Health and Social Science, The Hong Kong Polytechnic University, Hong Kong Special Administrative Region, People's Republic of China; [b]Department of Pathology, Princess Margaret Hospital, Hong Kong Special Administrative Region, People's Republic of China; [c]Department of Clinical Pathology, Pamela Youde Nethersole Eastern Hospital, Hong Kong Special Administrative Region, People's Republic of China; [d]Department of Clinical Pathology, United Christian Hospital, Hong Kong Special Administrative Region, People's Republic of China

ABSTRACT

During the COVID-19 pandemic, stringent public health measures led to historically low influenza activity in Hong Kong. However, after these interventions were relaxed in 2023, Influenza A viruses (IAV), including A(H1N1)pdm09 and A(H3N2), rapidly resurfaced. In this study, 1,046 clinical cases collected throughout 2023 underwent comprehensive genomic analysis using Oxford Nanopore Technologies (ONT). Phylogenetic analyses of the assembled genome segments were conducted alongside several global public sequences for comparison. The dataset is comprised of 593 A(H1N1)pdm09 sequences, predominantly of hemagglutinin (HA) subclade 5a.2a and neuraminidase (NA) subclade C.5.3, and 453 A(H3N2) sequences classified mainly as HA subclade 2a.3a.1 and NA subclade B.4.3. Phylogenetic comparisons revealed close genetic relationships between the studied viruses and 30 A(H1N1)pdm09 and 27 A(H3N2) sequences published in other regions during the same time. Additionally, identified amino acid substitutions may affect antigenicity and viral fitness. These findings underscore Hong Kong's high post–COVID–19 influenza diversity and the need for ongoing molecular surveillance to monitor emerging viral variants.

ARTICLE HISTORY Received 20 February 2025; Revised 15 May 2025; Accepted 13 June 2025

KEYWORDS Influenza A virus; A(H1N1)pdm09; A(H3N2); Nanopore sequencing; phylogenetic analysis; molecular epidemiology; non-pharmaceutical interventions (NPIs)

Introduction

Influenza is estimated to cause approximately 1 billion infections worldwide each year and results in 300,000 to 645,000 deaths, posing a significant threat to global health [1–3]. Endemic to many tropical regions, influenza results in seasonal outbreaks and epidemics. Occasionally, zoonotic transmission of novel influenza strains leads to pandemics [2].

Hong Kong, with a population of 7.4 million in Southern China, serves as a major international air travel and business hub, making it a critical sentinel site for monitoring the evolution and emergence of influenza. Historically, the city has endured multiple major influenza pandemics, including the devastating 1918–20 "Spanish Flu," the 1957–59 A(H2N2) outbreak, and the 1968–69 "Hong Kong Flu" A(H3N2) pandemic, all of which influenced its influenza surveillance and control measures [4–6] Due to intensive globalization, Hong Kong, a major gateway to Mainland China, was also affected by the 2009 A(H1N1) swine flu pandemic, the overall attack rate during the first wave was 10.7%, with the highest rates in children aged 5–14 years (43.4%) [7]. The strain now known as A(H1N1)pdm09 has become endemic and circulates annually. It has become the predominant seasonal A(H1N1) subtype and has been observed to repeatedly revert to its zoonotic origin in the swine population, posing a substantial risk for future outbreaks [2,8–10]. Therefore, it is important to understand viral evolution by performing

CONTACT Franklin Wang-Ngai Chow franklin.chow@polyu.edu.hk Department of Health Technology and Informatics, Faculty of Health and Social Science, The Hong Kong Polytechnic University, Y938, Block Y, 11 Yuk Choi Rd, Hung Hom, Hong Kong Special Administrative Region, People's Republic of China; Qing Xiong bear-qing.xiong@polyu.edu.hk Department of Health Technology and Informatics, Faculty of Health and Social Science, The Hong Kong Polytechnic University, Y938, Block Y, 11 Yuk Choi Rd, Hung Hom, Hong Kong Special Administrative Region, People's Republic of China; Gilman Kit-Hang Siu gilman.siu@polyu.edu.hk Department of Health Technology and Informatics, Faculty of Health and Social Science, The Hong Kong Polytechnic University, Y938, Block Y, 11 Yuk Choi Rd, Hung Hom, Hong Kong Special Administrative Region, People's Republic of China
*These authors contributed equally to this work.

Supplemental data for this article can be accessed online at https://doi.org/10.1080/22221751.2025.2521850.

subtype identification and phylogenetic analysis to detect the potential emergence of novel strains.

With clinical and public health resources heavily focused on SARS-CoV-2, detailed genomic analyses of influenza waned. As a result, there has been a lack of comprehensive whole-genome sequencing and variation analysis of influenza viruses in Hong Kong during and after COVID-19 [11]. Due to COVID-19 control measures, worldwide seasonal influenza activity decreased dramatically, with only sporadic cases detected in Hong Kong from 2020 to 2022 [12]. However, since the lifting of the mask mandate and other non-pharmaceutical interventions (NPIs) on the 1st of March 2023, a recurrence of influenza in Hong Kong has been observed. The development of third-generation sequencing, specifically Oxford Nanopore Technologies (ONT) sequencing, enables the generation of ultra-long reads, presents advantages over the current NGS standard and has been widely used to monitor the progression of the COVID-19 pandemic [13,14]. To enable real-time monitoring of viral evolution, facilitate early detection of novel strains, and provide crucial data for vaccine strain selection and public health response strategies, we collected influenza-positive respiratory specimens from Hong Kong, mainly in 2023, and applied ONT sequencing for long-read genomic analysis. This study first reports molecular variations of IAV in Hong Kong after the cessation of the mask mandate, revealing the subclades and evolutionary relationships of the main epidemic influenza in 2023.

Materials and methods

Samples collection

A total of 1,456 total nucleic acid samples were collected from the clinical microbiology laboratories of United Christian Hospital (UCH, Kowloon East Cluster), Pamela Youde Nethersole Eastern Hospital (PYNEH, Hong Kong East Cluster), and Princess Margaret Hospital (PMH, Kowloon West Cluster) between October 31, 2022, and May 30, 2024. The respiratory specimens used for genomic sequencing were residual materials collected during routine diagnostic testing. Specifically, the samples were obtained from in-patients from one-month to 101-years old who presented with influenza-like symptoms and were tested using the GeneXpert Infinity System with the Xpert® Xpress CoV-2/Flu/RSV Plus assay. Cases that tested positive for influenza with cycle threshold (Ct) value of < 25 were retrieved, and total nucleic acid was extracted using the NUCLISENS easyMAG system and sent to the lab for downstream Nanopore sequencing. Most samples were obtained through nasopharyngeal and throat swabs.

Oxford Nanopore Technologies (ONT) sequencing

Samples with sufficient volume remaining upon receipt and a FluA RT-qPCR (EUA/CDC method Luna® Probe One-Step RT-qPCR, NEB, USA) Ct value lower than or equal to 30 were sequenced. Gene segments of IAV in the samples were simultaneously amplified using a SuperScript III one-step RT–PCR system with Platinum Taq DNA Polymerase kit (Invitrogen, USA) according to the manufacturer's instructions with a 5.25 µL sample as input. A primer mix composed of Tuni-12, Tuni-12.4, and Tuni-13 was prepared for influenza A samples, while a FluB universal primer cocktail was made for samples positive for influenza B [15,16]. The thermocycling conditions were 60 min at 42°C, 2 min at 94°C, and then five cycles of 30 s at 94°C, 30 s at 45°C and 3 min at 68°C, followed by 35 cycles of 30 s at 94°C, 30 s at 57°C and 3 min at 68°C, with a final extension at 68°C for 2 min [15]. The amplified products were quantified using a Qubit 2.0 Fluorometer with a Qubit 1x dsDNA high-sensitivity assay kit (Thermo Fisher Scientific, USA).

Library preparation was done according to the manufacturer's instructions using the Rapid Barcoding Kit 96 (SQK-RBK110.96, Oxford Nanopore Technologies, UK). Briefly, 7.5 µL of the amplified products (100 ng) from each specimen were mixed with 2 µL of a unique rapid barcode. The mixture was incubated at 30°C for 2 min and then at 80°C for 2 min. A batch of 96 barcoded products, including a negative control, were pooled and purified using 1x AMPure XP beads (Beckman Coulter, USA). Elution was done with 15 µL of elution buffer after washing. Finally, 800 ng of the final library was loaded onto the FLO-MIN106D (R9.4.1) flow cell on a GridION platform (Oxford Nanopore Technologies, UK) for a 24-hour sequencing run.

Data processing

Raw nanopore read signals were automatically demultiplexed, barcode adapter-trimmed, and base-called with super-accurate base-calling (SUP) mode using Guppy (version 6.3.8, 6.4.6, or 6.5.7) with MinKNOW software (Oxford Nanopore Technologies, UK). The reads underwent quality control using NanoPlot (version 1.43.0) and were then filtered by Chopper (version 0.8.0) using a cut-off of a minimum length of 100 and a minimum average quality of 10 [17]. To further determine the HA and NA subtypes of each sequences, Mash (version 2.3) was used to screen the reads with the database built by the HA and NA sequences of IAV downloaded from the NCBI Influenza Virus Resource database [18]. FluStAR was also used to calculate each sequences's best-matched genomes and subtypes [19].

Primary screening divided the samples into A(H1N1)pdm09 or A(H3N2) subtypes. Unclassified sequences were further aligned to B/Brisbane/60/2008 (Victoria) and B/Wisconsin/01/2010 (Yamagata) to identify IBV lineages. The reads were then mapped using Minimap2 (version 2.28-r1209) to the reference genomes A/Human/New York City/PV81860/2022 for A(H1N1)pdm09 and A/Human/New York City/PV63281/2022 for A(H3N2) [20]. Sequencing coverage and depth for HA and NA segments were calculated using Samtools (version 1.21) and those with incomplete reads mapping coverage or an average mapping depth below 30x were filtered out in the subsequent analysis [21]. Bcftools (version 1.21) was used for calling variations and generating consensus genome sequences for each sample [21]. The indels were double-checked in IGV, and the SNPs with a quality score below Q30 were filtered. The genotype with the highest allelic depth at each multi-allelic site will be regarded as the consensus [22].

Phylogenetic analysis

In addition to the samples sequenced in this study, representative sequences of A(H1N1)pdm09 (n = 30) and A(H3N2) (n = 27), collected globally between the end of 2022 and the beginning of 2024, were downloaded from the GISAID database (Table S4). A stratified sampling strategy was employed to select data from a diverse range of countries and regions. Vaccine reference sequences for the 2022–2023 Northern Hemisphere influenza season were obtained from the NCBI database (accession numbers: OQ719014.1, OQ719015.1, OR533781.1, OR533783.1, OR567258.1, OR567121.1, OQ718998.1, and OQ718999.1). Complete coding sequences of the eight segments of IAV, along with published and vaccine sequences, were used to construct the phylogenetic trees. Additionally, the eight segments were concatenated in the order from PB2 to NS to construct concatenated trees, with one partition for each segment.

Multiple sequence alignments were performed using MAFFT (version 7.525) [23]. Maximum likelihood (ML) phylogenetic trees were constructed using RAxML (version 8.2.12) with 1000 bootstrap replicates [24]. The phylogenetic trees for A(H1N1)pdm09 and A(H3N2) were rooted with the WHO vaccine strains A/Victoria/2570/2019 and A/Darwin/9/2021, respectively. The PAML toolkit was used to optimize the trees and perform amino acid substitution analyses [25]. Subclades of the HA and NA segments were identified using Nextclade [26]. The phylogenetic trees were visualized with the ggtree package in R, and tanglegrams were constructed to illustrate the phylogenetic relationships between different segments and concatenated sequences using the dendextend package [27]. Hierarchical clustering of each gene segment was performed using rhierbaps (v 1.1.4) with the parameters set as max.depth = 2, n.pops = 20, and n.extra.rounds = 10, and the first-level clusters were utilized for reassortment identification [28,29].

Protein modelling structure prediction

The HA and NA amino acid sequences of the majority subclades of A(H1N1)pdm09 and A(H3N2) identified in this study were submitted to SWISS-MODEL for homology-based structure prediction [30,31]. The templates 7kna.1.A [H1 6B.1A.5a.2a], 2yp9.1.C [H3 3C.2a1b.2a.2a.3a.1], 5hug.1.A [N1 C.5.3], 7u4f.1.D [N2 B.4.3] were selected for modelling based on sequence identity and the GMQE (Global Model Quality Estimate) score [32–35]. The resulting models were annotated and visualized using ChimeraX version 1.8 [36].

Results

A total of 1,456 nucleic acid samples were collected in this study. Of these, 1,208 samples (83%) underwent ONT sequencing after excluding those with low volume. Reference mapping identified 593 (49%) A(H1N1)pdm09, 453 (38%) A(H3N2), and 30 (2%) influenza B viral infections for epidemiological analysis. To ensure sequence completeness and accuracy, strict criteria were applied to filter sequences for phylogenetic construction. As a result, 998 samples were included in the phylogenetic analysis of the HA and NA segments, while 795 samples were further selected for concatenated tree construction and subsequent analyses to ensure a high quality of the whole genome assembly (Table S1).

Epidemiological analysis

The collection dates of these samples were concentrated between weeks 11 and 29 of 2023, accounting for 85.9% of the cohort (Figure 1). By comparing these data with statistics from the Centre for Health Protection of the HKSAR government (blue line), the number of samples collected followed the same trend observed in citywide laboratory monitoring through week 30 of 2023, with both peaking in week 15. Following the lifting of Hong Kong's mask mandate, the last COVID-19 control measure, influenza cases surged rapidly on March 1, 2023.

A(H1N1)pdm09 was detected most frequently during the spring, between weeks 11 and 20, while A(H3N2) gradually increased, reaching a lagging peak in the summer. A small number of Influenza B virus (IBV) cases belonging to the Victoria lineage were primarily observed during the first two months

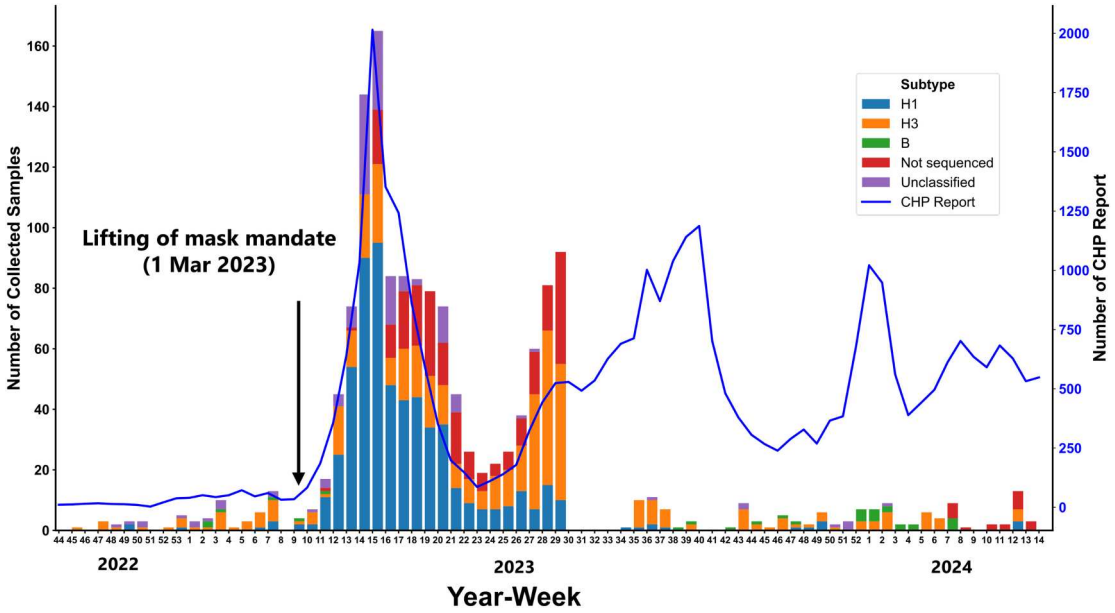

Figure 1. Virus samples sequenced and classified in this study by week. This graph shows the number of samples collected during this study by week. The blue and orange bars represent the identified Influenza A H1 and H3 subtypes, while the green bar represents Influenza B. The number of samples not sequenced due to quality control issues and those unclassified are also shown. The city-wide statistics on the total number of influenza cases, provided by the CHP, are plotted on the right y-axis with a blue broken line. The arrow shows the date of lifting of mask mandate.

of 2024 (Figure 1). No Yamagata lineage IBV was detected among the samples included in this study.

The demographics of sample sources show that the young and elderly have a stronger representation, forming the typical U-shaped age distribution (Figure S1). Adolescents and young adults (16 to 45 years old) accounted for only 8% (H1N1) and 18% (H3N2) of all cases, excluding a small number of unrecorded samples. The number of male patients is 31% (H1N1) and 59% (H3N2) higher than that of female patients. This is likely due to higher admission rates for the more vulnerable, driven by an increased likelihood of developing complications from influenza infections and other preferences in seeking medical attention.

Phylogenetic analysis

The raw reads of IAV samples were filtered and assembled into eight segments using a reference-based strategy. After removing sequences with low quality in continuity and mapping depth, 563 A(H1N1)pdm09 and 435 A(H3N2) sequences were retained for subsequent analyses (Table S2). The HA and NA segments were submitted to Nextclade for subclade identification. The prevalence trends of different HA subclades are shown in Figure 2.

Between October 2022 and February 2023, while mandatory mask mandate and other NPIs were still in effect, a small number of influenza cases were reported, most of which were attributed to A(H3N2). Multiple H3 gene subclades were detected, with 3C.2a1b.2a.2a.1b being the most predominant. The surge in cases driven by A(H1N1)pdm09 began in March and peaked in mid-April 2023 with the major HA subclade 6B.1A.5a.2a. Subsequently, A(H3N2) regained predominance in July 2023, marked by the emergence of HA subclade 3C.2a1b.2a.2a.3a.1.

To further elucidate the phylogeny of locally circulating IAV strains, ML trees were constructed using HA and NA sequences, along with 30 global A(H1N1)pdm09 sequences, 27 global A(H3N2) sequences collected from the GISAID databases during the same period, and four vaccine strains from the 2022–2023 Northern Hemisphere influenza season (Table S3). Additionally, multi-gene phylogenetic trees constructed from concatenated sequences revealed genome-wide diversity.

For Influenza A(H1N1)pdm09, the HA (Figure 3) and NA (Figure 4) phylogenetic trees exhibit similar overall topologies, although their subclade compositions differ. For the H1 gene, the vaccine strains were identified as belonging to the 6B.1A.5a.2 subclade, while all collected and published sequences were classified into 6B.1A.5a.2a and 6B.1A.5a.2a.1 during the study period. Notably, 6B.1A.5a.2a was predominant during the spring 2023 epidemic, while the 6B.1A.5a.2a.1 subclade, representing around 20% of cases later in July 2023, formed a distinct branch. The N1 genes displayed multiple subclades, with the vaccine strains classified under the B.3 subclade. Notably, subclade C.5.3 was the most prevalent, accounting for approximately 90% of the sequences. The phylogenetic tree indicates that C.5.3, along with its secondary branches (C.5.3.1 and C.5.3.2), diverged from a

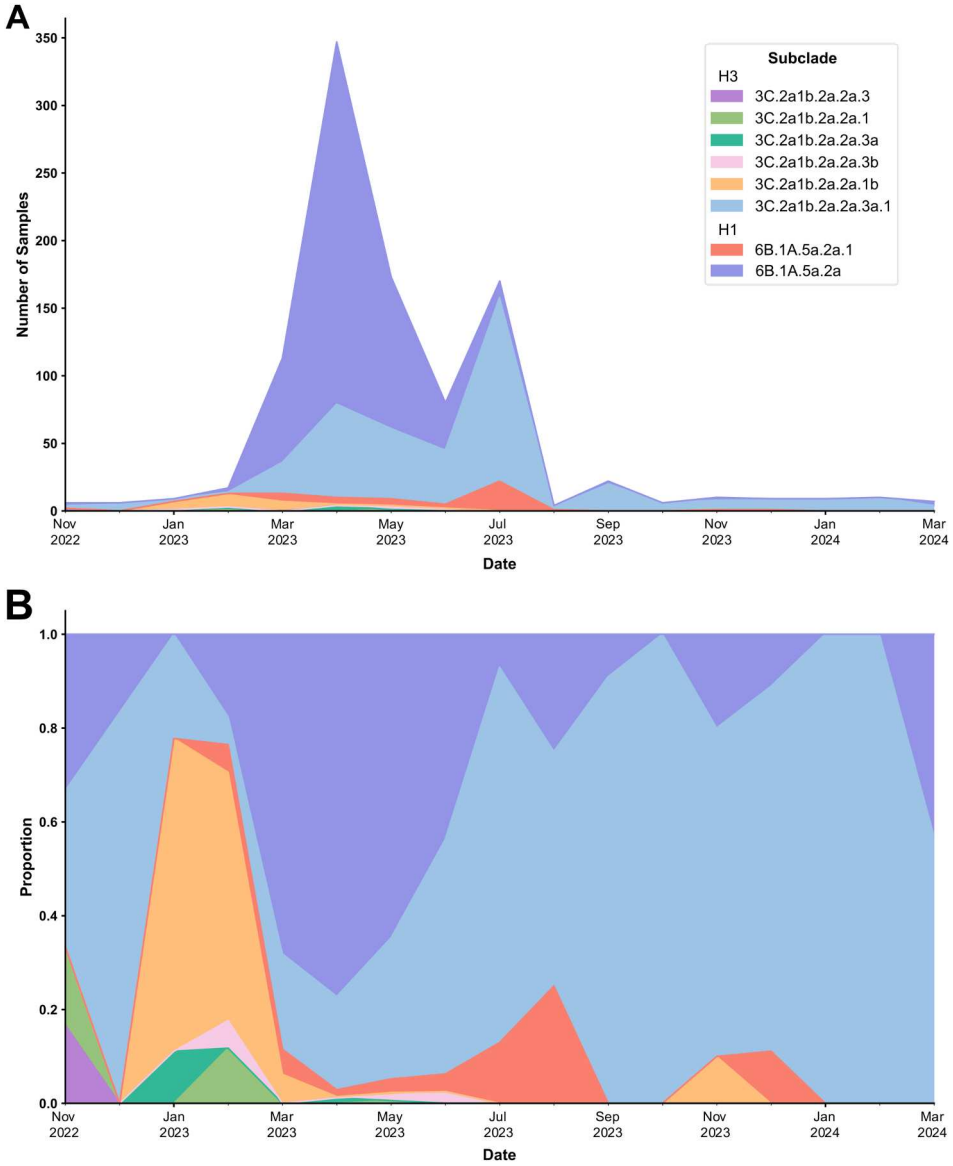

Figure 2. Subclade distribution of HA sequences by month. The panels show the (A) number and (B) proportion of IAV subclades from both H1 and H3 subtypes identified from November 2022 to March 2024. Subclades 6B.1A.5a.2a.1 and 6B.1A.5a.2a belong to the H1 subtype, while other subclades belong to the H3 subtype.

common ancestor within the cluster of subclade C. By comparing the phylogeny of published sequences, the majority of A(H1N1)pdm09 sequences from this study clustered closely with samples from Mainland China and Europe in both the H1 and N1 genes. However, published sequences were more widely distributed on branches closer to the root and tended to exhibit longer branch lengths. Notably, one Hong Kong sample from GISAID collected in 2023 showed a high degree of similarity to the sequences from this study in both H1 and N1 genes. The Hong Kong sequences demonstrated significantly shorter branch lengths, indicating that the genetic characteristics of IAV in Hong Kong are highly consistent and independently verify our analysis.

The phylogenies of the all eight segments of A(H1N1)pdm09 are shown in Figure S2. Many identical sequences are observed in both the HA and NA trees, which exhibit smaller differences compared to the concatenated genome segments tree (Figure 5), reflecting the genome-wide diversity of the viruses. In the whole-genome phylogenetic tree, the topology is similar to the HA tree. However, subclade 6B.1A.5a.2a.1 no longer maintains complete monophyly and shows a shorter branch length. This indicates that the high mutation rate characteristic of this subclade is less prominent in sequences outside the HA segment. Notably, no evidence of intra-subtype reassortment was observed in either the SNP clustering (Figure 5) or the tanglegram analysis (Figure S4).

For Influenza A(H3N2), the H3 sequences predominantly belong to subclade 3C.2a1b.2a.2a.3a.1 (Figure 6), while the N2 genes were divided into subclades B.4 and B.4.3 (Figure 7). The vaccine strains were identified as part of subclade 3C.2a1b.2a.2a for

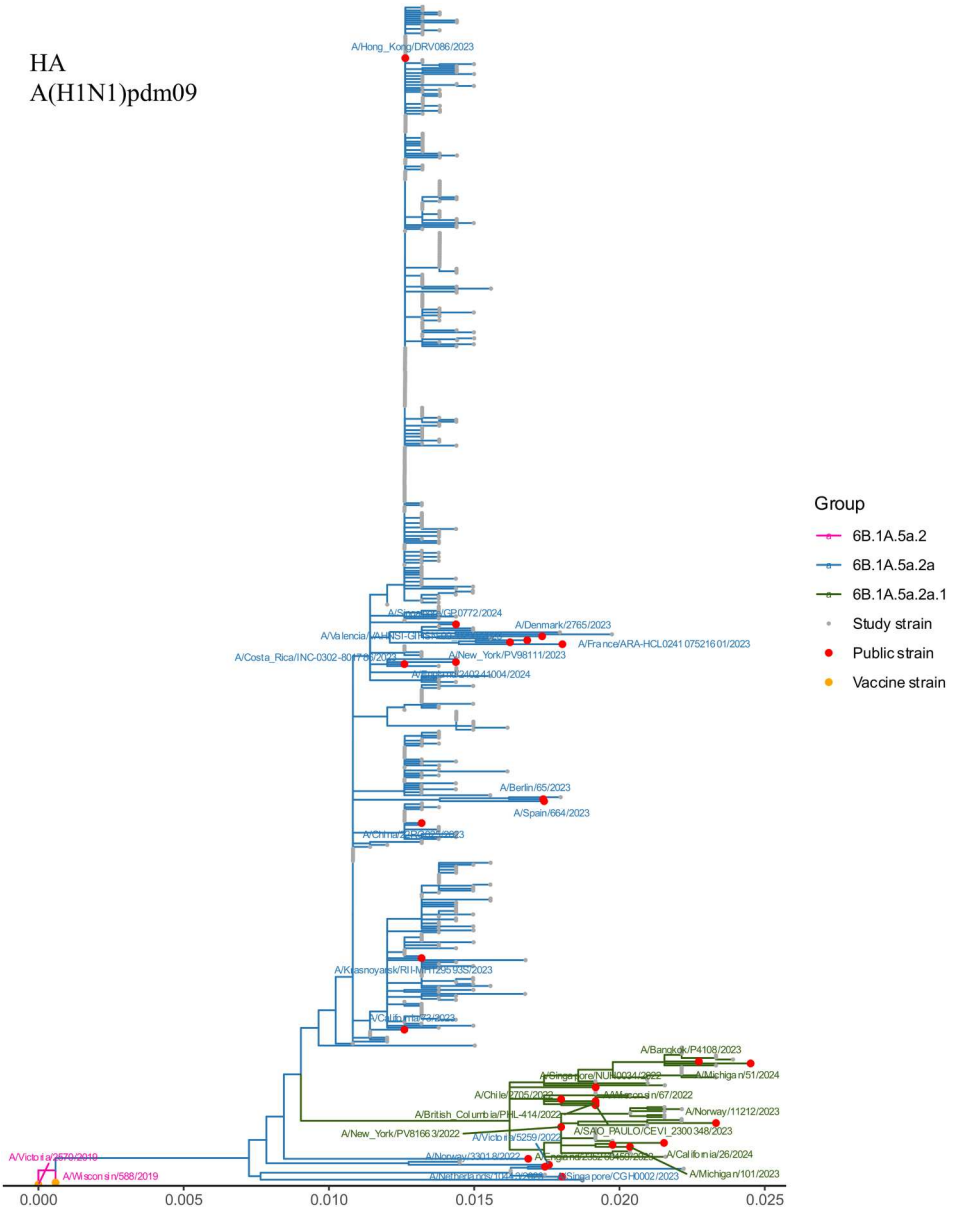

Figure 3. HA gene phylogeny of Influenza A(H1N1)pdm09 viruses. The ML tree for the 563 HA genes of A(H1N1)pdm09 analyzed in this study is shown, along with 29 published sequences from the GISAID database and two vaccine strains. The tree is rooted at the vaccine strain A/Victoria/2570/2019. Branches representing the three identified HA subclades are colour-coded. Nodes corresponding to published sequences are highlighted in red, representative sequences are labelled.

H3. Published sequences were grouped into two distinct branches within 3C.2a1b.2a.2a.3a.1: one group included samples from Texas, Chile, and Pakistan, while the other included sequences from the Czech Republic, Japan, and the Philippines. For N2, the sequences were divided into two distinct groups: one group was in mixed branches of B.4, B.4.1, and B.4.2, while the other group was clustered in B.4.3 at the top of the tree. The two A(H3N2) vaccine strains differed from one another and were closely related to some earlier-branching Hong Kong strains.

Unlike A(H1N1)pdm09, the concatenated genome phylogenetic tree of A(H3N2) reveals that the dominant HA clade 3C.2a1b.2a.2a.3a.1 splits into two branches, with one branch undergoing rapid evolution characterized by a higher rate of mutations (Figure 8). This divergence is likely influenced by the PB2, PA, and NP segments which exhibits great variation compared to other segments. In contrast the M and NS segments appear to remain relatively conserved (Figure S3). Similarly, the segment cluster and tanglegram of A(H3N2) do not show large-scale recombination. (Figure 8 and Figure S5)

Amino acid substitution analysis and protein modelling

The full-length coding sequences of the HA and NA segments were translated into protein sequences and compared to the vaccine strain for the 2022–2023 Northern Hemisphere flu season to explore further the amino acid divergence leading to the formation

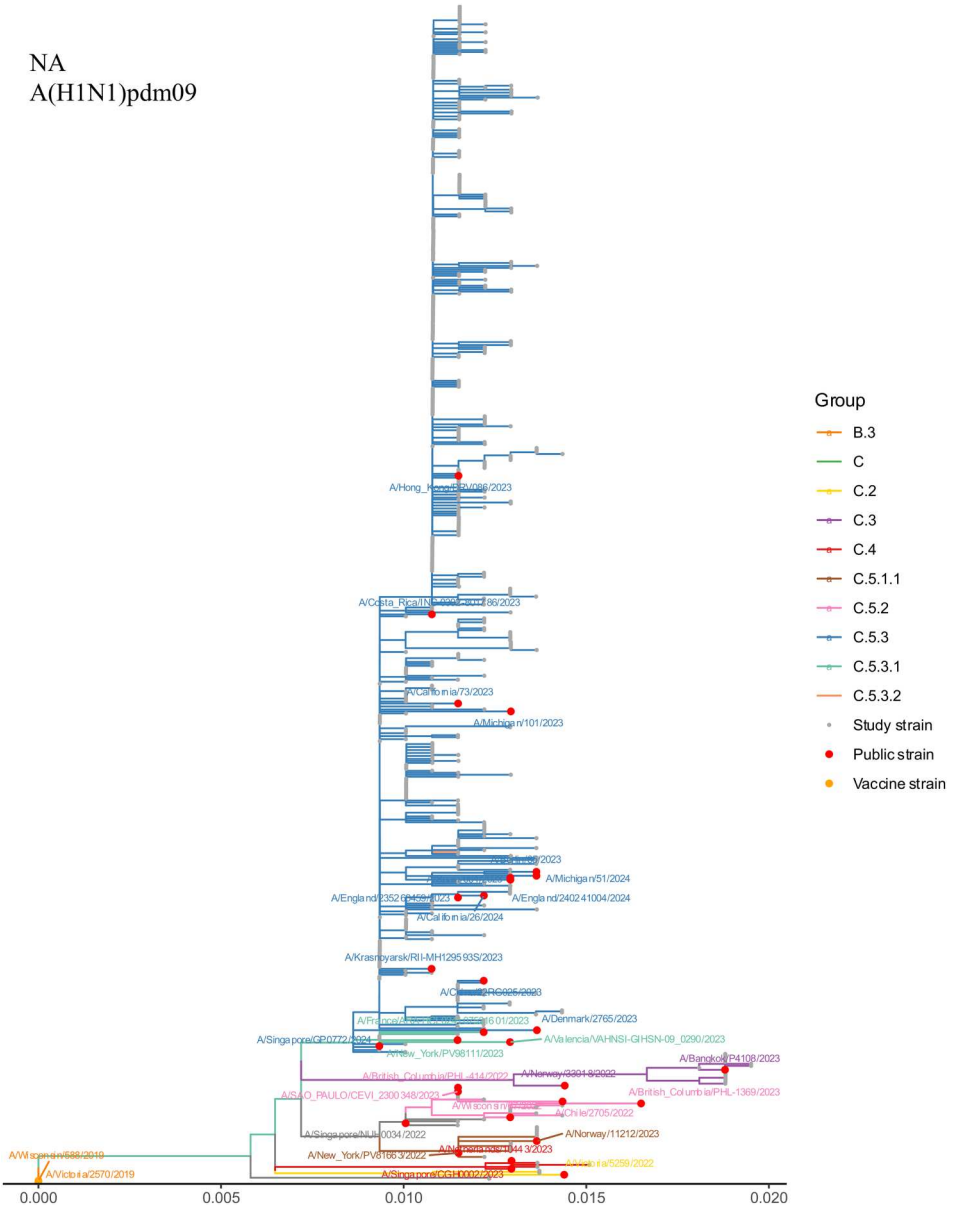

Figure 4. NA gene phylogeny of Influenza A(H1N1)pdm09 viruses. The ML tree for the 563 NA genes of A(H1N1)pdm09 analyzed in this study is shown, along with 30 published sequences from the GISAID database and two vaccine strains. The tree is rooted at the vaccine strain A/Victoria/2570/2019. Branches representing the 10 identified NA subclades are colour-coded. Nodes corresponding to published sequences are highlighted in red, representative sequences are labelled.

of various subclades. Several key amino acid substitutions in HA and NA were classified by subclades (Table 1).

Compared with the reference vaccine strain A/Victoria/2570/2019 (for H1N1), the Hong Kong A(H1N1)pdm09 viruses generally exhibited the substitutions K71Q, A203T, Q206E, R240Q, E241A, R276K, and K325R in the HA1 domain, which also contains the receptor-binding domain (RBD). These substitutions were primarily located in the "head" region of the HA protein, facing outward and away from the RBD pocket, while residing in major antigenic sites. The I435 V mutation in the HA2 subunit and K325R substitution in the HA1 subunit were in the "stalk" region of the HA protein near the transmembrane region (Figure 9, panels A and B). Additionally, the 5a.2a.1 subclade displayed as many as seven new substitutions compared to 5a.2a, but it lost the H416N substitution. (Table 1) In the NA sequences, which contain the active site responsible for sialic acid cleavage during viral egress, two substitutions at the 3' end of the head domain, V453M and K469N, were the most common amino acid changes observed, particularly in the subclade C.5.3 (n = 508). These changes, along with the widely reported S200N substitution, were all located on the protein's surface and may play a role in immune evasion (Figure 9, panels C and D). Other subclades also exhibited specific amino acid substitution patterns in the head domain, such as I195V and R257K in subclade C.3.

For A(H3N2) viruses, the HA sequences frequently displayed substitutions located in similar regions to

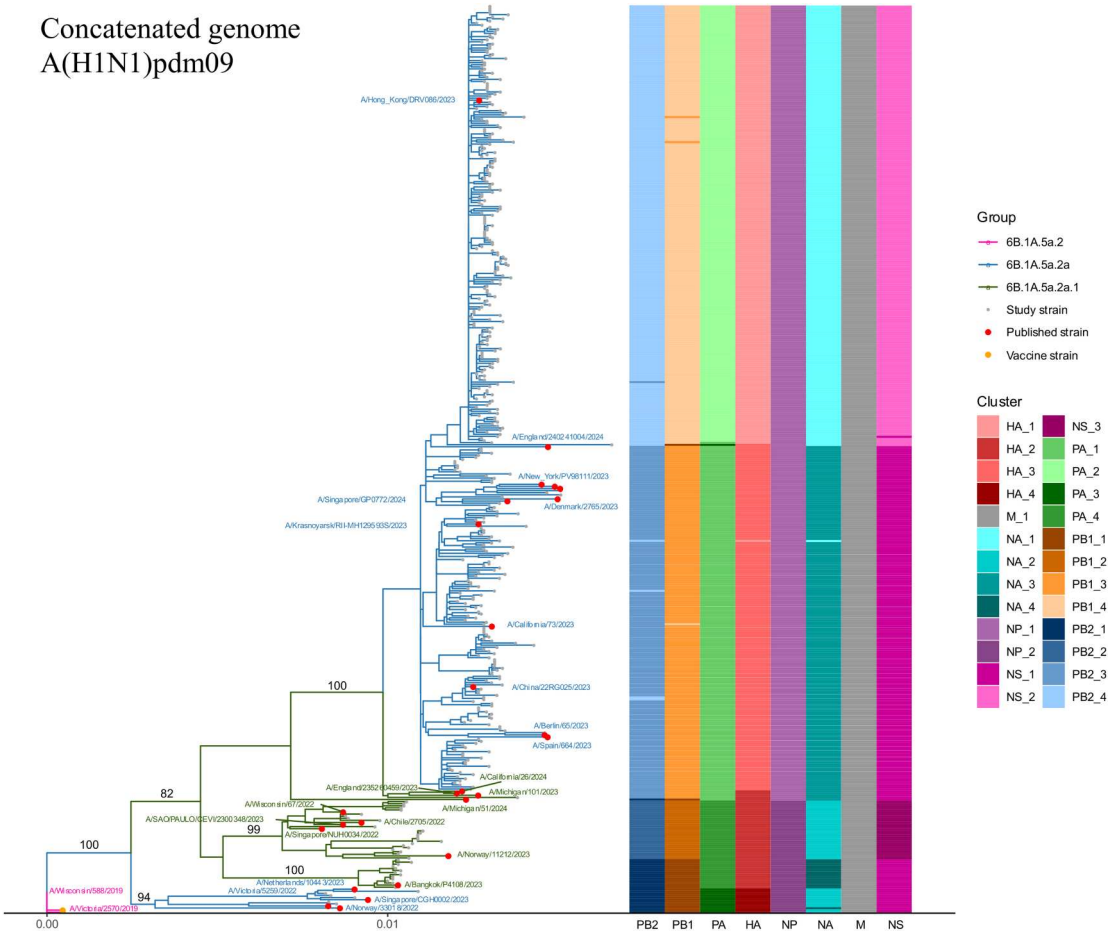

Figure 5. Concatenated genome segments phylogeny of Influenza A(H1N1)pdm09 viruses. The ML tree for the 407 concatenated genome segments of A(H1N1)pdm09 (left) and a cluster heatmap of the eight influenza genome segments (right) analyzed in this study. The tree includes strains from this study, 26 published sequences from the GISAID database, and two vaccine strains. It is rooted at the vaccine strain A/Victoria/2570/2019. The branches corresponding to the three identified HA subclades are colour-coded in the ML tree. Nodes representing published sequences are highlighted in red, and representative sequences are labelled. Influenza genome segments were clustered by single nucleotide polymorphisms (SNPs) and are visualized using a colour scale.

those identified in A(H1N1)pdm09, potentially playing a role in immune evasion while conserving their function for receptor binding (Figure 9, panels E and F). Notable substitutions included D69N, N202D, and G241D in subclade 3C.2a1b.2a.2a.3a.1, which had the highest sample count (n = 395). Similarly, the NA sequences showed consistent substitutions, including S150H and S331G, across multiple subclades, with subclade B.4.3 having the largest sample size (n = 269). These changes were also located on the protein's surface and did not affect sialic acid cleavage (Figure 9, panels G and H). These patterns highlight specific evolutionary changes within the A(H3N2) viruses.

Discussion

This study collected 1,456 clinical influenza samples in Hong Kong, China, primarily from week 44 (October) of 2022 to week 29 (May) of 2024. Our data followed the development of influenza case trends in the city, capturing approximately 10% of the citywide laboratory-monitored influenza cases reported [37]. This period allowed us to track the delayed onset of the 2023 flu season, which started several months later than in previous years, because of the suspension of COVID-19 public health interventions. We documented two surges of Influenza A cases: first by A(H1N1)pdm09 and then by A(H3N2). While a notable discrepancy exists between our data collection and actual citywide cases after week 30 of 2023, the overall temporal trends of both Influenza A subtypes were characterized. The prevalence of Influenza A (n = 1,046) was significantly higher than that of Influenza B (n = 30), dominating the epidemic during this influenza season. Of these Influenza A cases, H1 (n = 593) slightly outnumbered H3 (n = 453). All identified Influenza B lineages belonged to the B/Victoria lineage, supporting the conjecture that the Yamagata lineage has been extinct since 2020 [38]. These findings align with global WHO statistics during the same period [39].

Following the broad implementation of public health interventions to curb the spread of SARS-CoV-2, the virus that causes COVID-19, the circulation of the influenza virus in Hong Kong and other regions worldwide fell to historically low levels. Similarly, during the

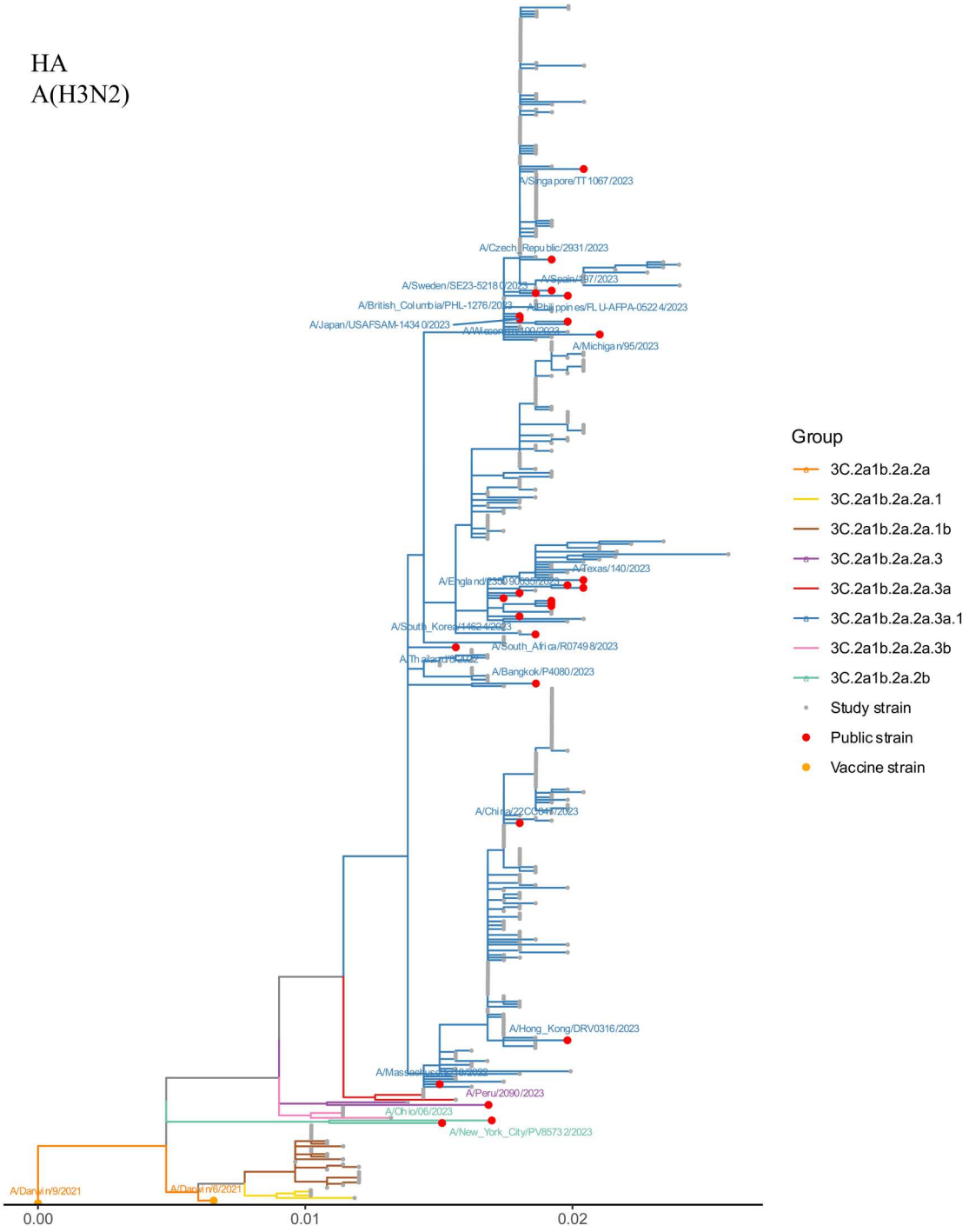

Figure 6. HA gene phylogeny of Influenza A(H3N2) viruses. The ML tree for the 435 HA genes of A(H3N2) analyzed in this study is shown here, along with 27 published sequences from the GISAID database and two vaccine strains. The tree is rooted at the vaccine strain A/Darwin/9/2021. The branches for the eight identified HA subclades are colour-coded. Nodes corresponding to published sequences are highlighted in red, representative sequences are labelled.

implementation of public health and social measures (PHSM) for COVID-19, cases of influenza virus declined by 60-80% in countries such as the United States, Singapore, Mexico, and New Zealand [40]. As a natural phenomenon, adaptive immunity previously gained through vaccination or exposure diminishes over time without occasional challenges [41,42]. Limited exposure to seasonal influenza and other respiratory viruses during the pandemic has also left young children more vulnerable [43]. A low influenza vaccination rate and a mismatch in vaccine strain could lead to major epidemics, as a significant portion of the population is immunogenically naive [43,44].

Pursuing a "zero infection" goal, Hong Kong implemented stringent measures – including restrictions on group gatherings, flight bans, extended hotel quarantines for travellers, school closures, and one of the world's longest mask mandate (July 2020 to March 2023) – which greatly suppressed endemic respiratory viruses including IAV [45]. However,

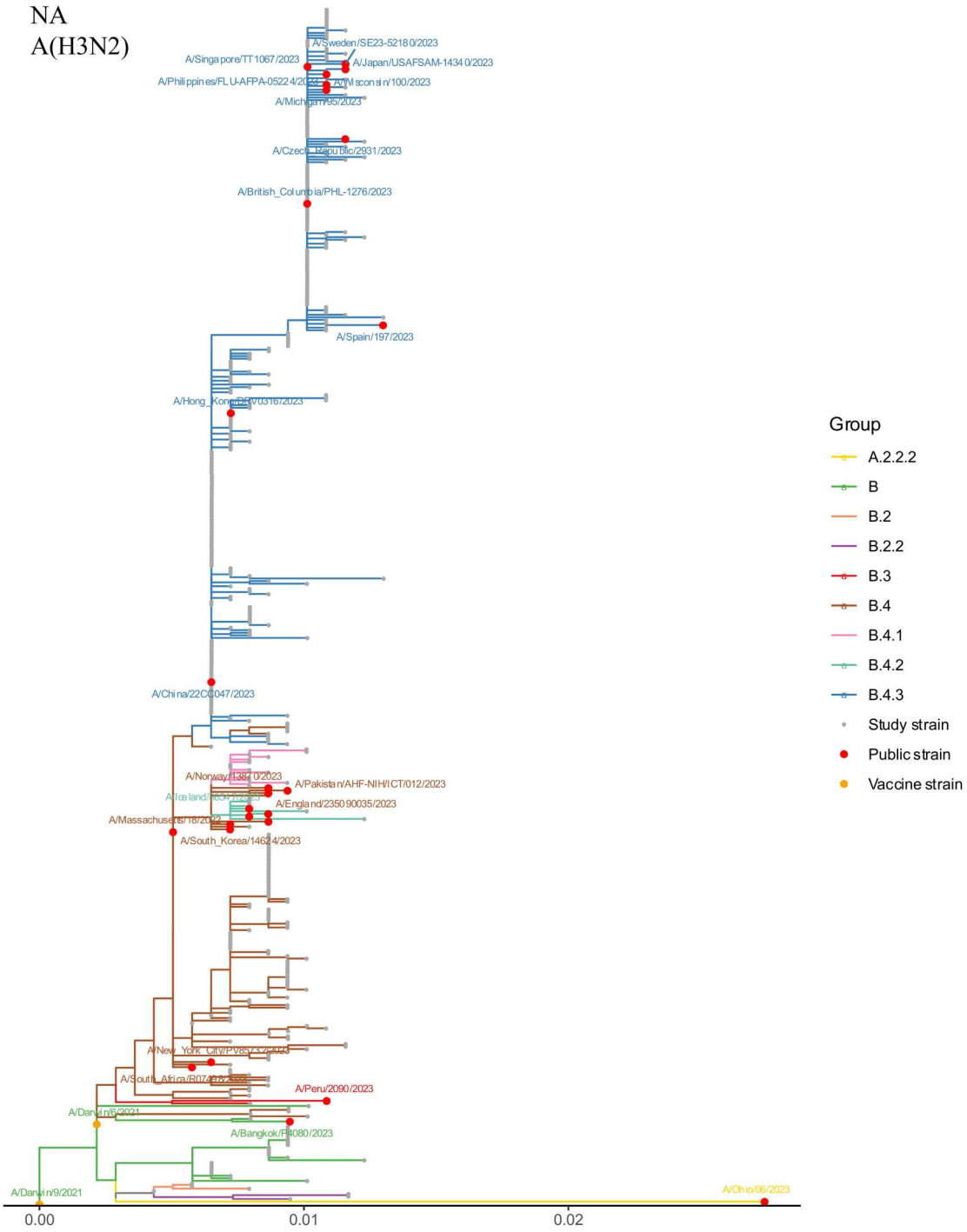

Figure 7. NA gene phylogeny of Influenza A(H3N2) viruses. The ML tree for the 435 NA genes of A(H3N2) analyzed in this study is shown here, along with 26 published sequences from the GISAID database and two vaccine strains. The tree is rooted at the vaccine strain A/Darwin/9/2021. The branches for the nine identified NA subclades are colour-coded. Nodes corresponding to published sequences are highlighted in red, representative sequences are labelled.

following the cessation of the mask mandate in March 2023, the city experienced a surge in influenza and other non-influenza respiratory virus (NIRV) infections. This surge deviated from the usual "winter influenza season" that typically begins in late December and ends in March and was dominated by IAV, aligning with the patterns before the COVID-19 pandemic (2016/17, 2018/19, and 2019/20) [46,47]. At the same time, the relaxation of such NPIs may lead to a resurgence of respiratory viruses that could exhibit non-seasonal patterns [48,49]. These findings highlight the need for ongoing surveillance of circulating strains and provide insights into the dynamics of viral transmission and evolution in response to prolonged NPIs.

Phylogenetic analysis revealed that the genome of the 2023 Hong Kong IAV strains was highly uniform, with the dominant subclade 6B.1A.5a.2a of the HA segment and subclade C.5.3 of the NA segment accounting for 92% and 90% of A(H1N1)pdm09

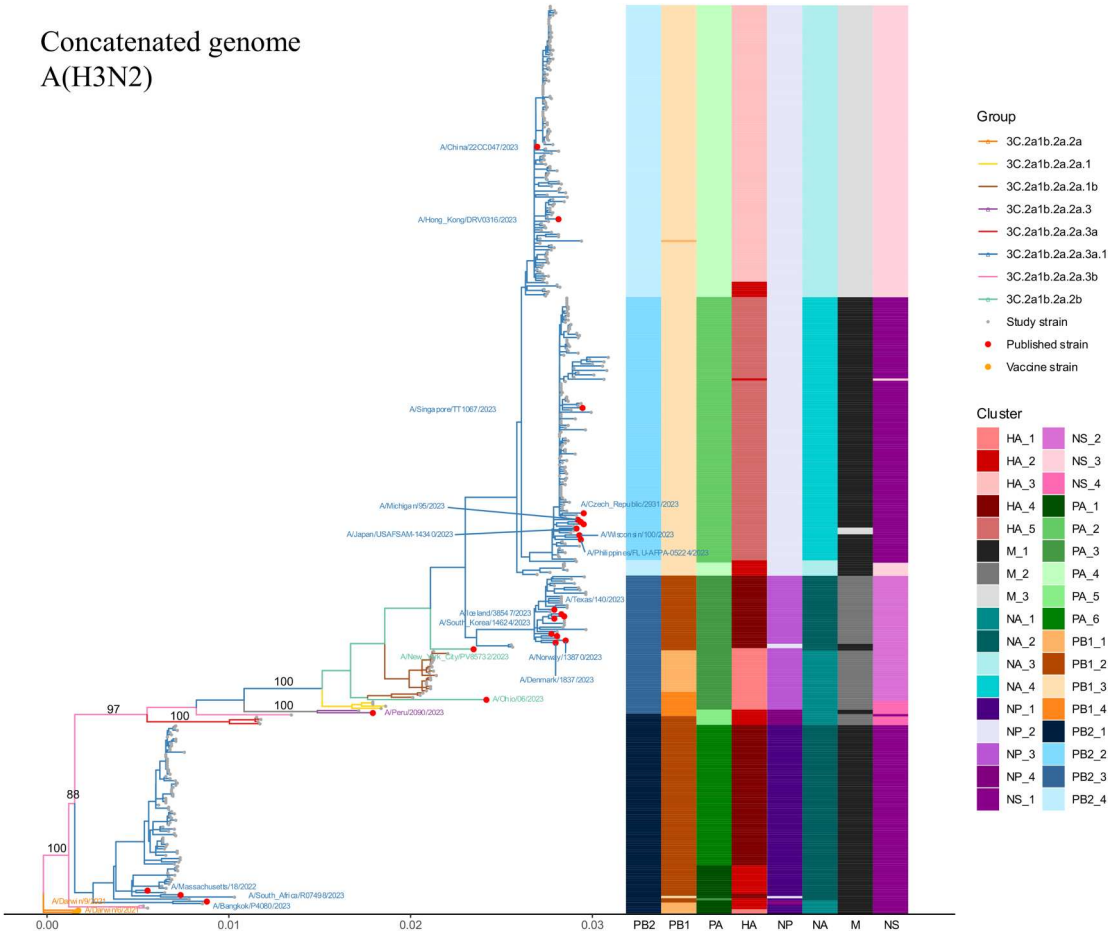

Figure 8. Concatenated genome segments phylogeny of Influenza A(H3N2) viruses. The maximum likelihood (ML) tree for the 388 concatenated genome segments of A(H3N2) (left) and a cluster heatmap of the eight influenza genome segments (right) analyzed in this study. The tree includes strains from this study, 24 published sequences from the GISAID database, and two vaccine strains. It is rooted at the vaccine strain A/Darwin/9/2021. The branches corresponding to the three identified HA subclades are colour-coded in the ML tree. Nodes representing published sequences are highlighted in red, and representative sequences are labelled. Influenza genome segments were clustered by single nucleotide polymorphisms (SNPs) and are visualized using a colour scale.

cases, respectively. In contrast, the A(H3N2) virus exhibited greater genetic diversity, particularly in the NA segment, which was represented by two main subclades (B.4 and B.4.3). By comparing the topology of the four phylogenetic trees and the distribution of published sequences, we found that Hong Kong strains of A(H1N1)pdm09 were highly consistent and forms a pronounced subclade. In contrast, A(H3N2) exhibited higher within-city variation and heterogeneity. According to the global public dataset in GISAID, the two subclades of H1 detected in this study, 6B.1A.5a.2a and 6B.1A.5a.2a.1 emerged at the end of 2021 and expanded in the 2022–2023 Northern Hemispheres flu season. Similarly, the six subclades of H3 detected in this study also followed the temporal characteristics of H1. The major subclades, namely, 6B.1A.5a.2a for H1 and 3C.2a1b.2a.2a.3a.1 for H3, were responsible for the epidemic in 2023 and 2024. These patterns reflect that the IAV strains detected in Hong Kong during 2023 were highly consistent with global observations and genetically different from pre-COVID-19 influenza pandemics.

Vaccine effectiveness (VE) studies conducted during this period observed decreased protection for patients between June and November 2023, suggesting a mismatch between the selected vaccine strains and the actual circulating strains in the local community, potentially due to antigenic drift events [37]. Our large-scale sequencing and evolutionary analysis provide crucial insights into the genetic basis for this reduced VE. The identified amino acid substitutions in both A(H1N1)pdm09 and A(H3N2) viruses, particularly within the HA and NA proteins, likely contributed to the observed antigenic drift. For A(H1N1)pdm09, the accumulation of substitutions in the HA1 head region, specifically K71Q, A203T, Q206E, R240Q, E241A, R276K, and K325R, is significant. While these changes are located outside the receptor-binding domain (RBD) pocket, their position within major antigenic sites suggests a role in altering antigenicity and potentially impacting antibody binding, thereby reducing vaccine-induced immunity. In the NA protein of A(H1N1)pdm09, the prevalent V453M and K469N substitutions, along with the

Table 1. Amino acid substitutions identified for the HA and NA gene of two Influenza A types against the 2022–2023 vaccine strains: A/Victoria/2570/2019(H1N1) and A/Darwin/9/2021(H3N2). Effective mutation sites previously identified in other studies were underlined.

Type	Segment	Subclade	Number	Representative amino acid substitutions
A(H1N1)pdm09	HA	6B.1A.5a.2a	519	K71Q, A203 T, Q206E, R240Q, E241A, R276K, K325R, H416N, I435V
		6B.1A.5a.2a.1	44	K71Q, P154S, K159R, A203 T, Q206E, T233A, R240Q, E241A, R276K, D277E, T294A, K325R, E373D, I435V, N468H
	NA	C	2	S200N, S247N, V346I, V453M
		C.2	2	S95N, N189S, D449N, V453M, K469M
		C.3	15	I195 V, I216 V, R257K, V453M, K469N
		C.4	4	I29M, V80M, I264T, I396M, V453M
		C.5	3	S339L, V453M, K469N
		C.5.1.1	14	S35N, N50D, G382E, V453M, K469N
		C.5.2	11	I13V, S339L, V453M, K469N
		C.5.3	508	S200N, V453M, K469N
		C.5.3.1	3	S200N, I264T, V453M, K469N
		C.5.3.2	1	N73S, S200N, V453M, K469N
A(H3N2)	HA	3C.2a1b.2a.2a.1	4	D69G, D120G, N202D, G241D, K292R
		3C.2a1b.2a.2a.1b	25	D69G, D120G, I156K, N202D, G241D, K292R, R315K
		3C.2a1b.2a.2a.3	1	D69N, N112S, T151K, I156K, S161N, N202D, I208F, G241D, N394S, N505T
		3C.2a1b.2a.2a.3a	5	E66K, D69N, N112S, T151A, N202D, I208F, I239V, G241D, N394S
		3C.2a1b.2a.2a.3a.1	395	T3A, E66K, D69N, N112S, N138D, I156K, N202D, I208F, I239V, G241D, N394S, V521I
		3C.2a1b.2a.2a.3b	5	D69N, N112S, I156M, N202D, I208F, G241D, N394S
	NA	B	6	L140I, S150R, K328R, I469T
		B.2	26	S150R, D346G, R400K
		B.2.2	3	A82E, D127E, S150R, N234D, T238A, D346G
		B.3	1	S44P, L140I, S150R, H310R, S329N, S331R
		B.4	110	S150H, I469T
		B.4.1	14	S150H, K308R, I469T
		B.4.2	6	S150H, R400K, I469T
		B.4.3	269	S150H, S331G, I469T

previously reported S200N, are all surface-exposed, further supporting their potential role in immune evasion by altering antibody recognition. Similarly, the A(H3N2) viruses exhibited substitutions in analogous regions of the HA and NA protein, mirroring the patterns observed in A(H1N1)pdm09 and further reinforcing the role of antigenic drift in reduced vaccine effectiveness.

In this study, we found no significant evidence of intra- or inter-subtype reassortment among influenza virus segments. Although phylogenetic analysis identified minor clustering discrepancies in some sequences from a limited subset of samples (such as the HA of certain A(H3N2) reference strains), these observations likely reflect technical limitations inherent to short segments and the differential sensitivity of SNP-based clustering methods across segments, rather than true biological reassortment.

By comparing the recently reported Effective Mutations sites (EMs) list, we identified the amino acid substitutions highly associated with epitope or physiochemical property changes (Underlined in Table 1) [50,51]. Besides, future functional and modelling studies of influenza proteins should consider mutations that are rarely reported before the COVID-19 pandemic but are highly conserved among the subclades in this study, including V453M, K469N in N1, D69G/N, N112S, N394S in H3, and I469T in N2. Notably, amino acid substitutions G202D and D206N in the HA gene of A(H3N2), which have been reported to affect the virus's transmissibility, were also observed in the dominant subclade in this study [52]. However, the molecular mechanisms underlying most observed site variations remain unclear. These findings suggest that vaccines based on these strains may have had reduced effectiveness in preventing influenza infection during that year.

The current study surveyed locally circulating influenza viral strains and successfully characterized their genetic and evolutionary features. However, it was constrained by the intrinsic challenges of ONT sequencing, which reduced the reliability of deeper analyses related to single nucleotide polymorphisms (SNPs), viral recombination, and co-infection events. Despite these drawbacks, ONT still offers rapid genomic surveillance during the outbreak/winter surge of influenza, benefiting public health research and policymaking. Additionally, the virological and immunological effects of the observed amino acid substitutions were assessed only *in silico* and remain unverified experimentally. Future studies should, therefore, include functional investigations to elucidate the biological significance of these substitutions while also improving sequencing accuracy and data resolution to better capture viral evolution and host interactions. Such efforts will be crucial to advancing our understanding of influenza virus adaptation and informing more effective surveillance and vaccine strategies.

Conclusion

This study provides a detailed genomic and epidemiological characterization of Influenza A viruses

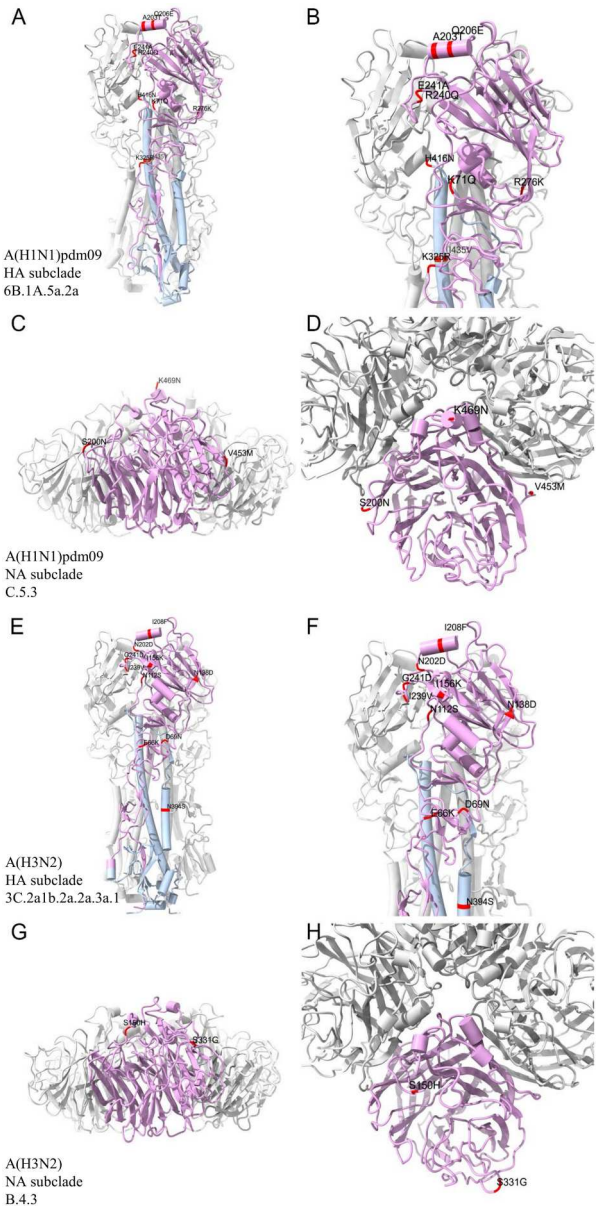

Figure 9. Three-dimensional homology models of HA and NA proteins from prevalent Influenza A subclades. (A, B) HA model for A(H1N1)pdm09 subclade 6B.1A.5a.2a. (C, D) NA model for A(H1N1)pdm09 subclade C.5.3. (E, F) HA model for A(H3N2) subclade 3C.2a1b.2a.2a.3a.1. (G, H) NA model for A(H3N2) subclade B.4.3. For clarity, only one monomer is highlighted and labelled within each complex. Solvents and ligands are omitted, and α-helices are represented as tubes. Shadows and transparency are applied to enhance depth perception. In the HA models, HA1 domains are shown in plum, and HA2 domains are shown in light blue. Identified substitutions are labelled, with residue locations highlighted in red. Panels (A) and (E) show full HA structures, with the transmembrane region oriented downward, while panels (B) and (F) provide zoomed-in views highlighting the identified substitutions. For the NA models, only the head domain is displayed due to template availability. Panels (C) and (G) show side views, while panels (D) and (H) show top-down views.

circulating in Hong Kong during the 2022–2023 flu season, capturing the delayed onset of the flu season and documenting the dominance of A(H1N1)pdm09 and A(H3N2) subtypes. Despite differences in genetic diversity – A(H3N2) appeared more heterogeneous, while A(H1N1)pdm09 was relatively homogenous – both subtypes displayed amino acid substitutions potentially linked to transmissibility and immune evasion, underscoring the potential impact of antigenic drift on vaccine effectiveness. These findings emphasize the continued need for vigilant surveillance and adaptable vaccine strategies to mitigate the public health burden of influenza in the post-COVID-19 pandemic era and prepare for potential future epidemics.

Acknowledgements

We thank the Departments of Pathology at Princess Margaret Hospital, Clinical Pathology at Pamela Youde Nethersole Eastern Hospital, and Clinical Pathology at United Christian Hospital, all within the HKSAR, China, for their support in sample collection, data provision, and expert opinions.

Disclosure statement

No potential conflict of interest was reported by the author(s).

Funding

The Health and Health Services Research Fund of the Health Bureau of the HKSAR government partly supported this work. (ref. 24230402).

Ethics statement

The current study utilizing leftover respiratory samples from clinical testing was approved by the Hong Kong Hospital Authority Central IRB (ref. no. CIRB-2024-122-1).

Data availability statement

The nanopore sequencing data of IAV used in this study are deposited in the Sequence Read Archive (SRA) of the NCBI database under BioProject PRJNA1213174.

ORCID

Jingyuan Bian http://orcid.org/0009-0003-5239-7046
Joshua Fung http://orcid.org/0000-0002-5817-8456
Cyrus Ka-Wo Wong http://orcid.org/0009-0006-4042-7529
Bei Jiang http://orcid.org/0009-0004-3176-4983
Miranda Chong-Yee Yau http://orcid.org/0009-0004-3211-2020
Qing Xiong http://orcid.org/0000-0001-6000-4677
Gilman Kit-Hang Siu http://orcid.org/0000-0002-4354-3393
Franklin Wang-Ngai Chow http://orcid.org/0000-0003-1275-2464

References

[1] Stohr K. Influenza–WHO cares. Lancet Infect Dis. 2002;2:517. doi:10.1016/s1473-3099(02)00366-3

[2] Krammer F, Smith GJD, Fouchier RAM, et al. Influenza. Nat Rev Dis Primers. 2018;4:3. doi:10.1038/s41572-018-0002-y

[3] Iuliano AD, Roguski KM, Chang HH, et al. Estimates of global seasonal influenza-associated respiratory mortality: a modelling study. Lancet. 2018;391:1285–1300. doi:10.1016/S0140-6736(17)33293-2

[4] Ho PL, Chow KH. Mortality burden of the 1918-1920 influenza pandemic in Hong Kong. Influenza Other Respir Viruses. 2009;3:261–263. doi:10.1111/j.1750-2659.2009.00105.x

[5] Viboud C, Simonsen L, Fuentes R, et al. Global mortality impact of the 1957-1959 influenza pandemic. J Infect Dis. 2016;213:738–745. doi:10.1093/infdis/jiv534

[6] Viboud C, Grais R, Lafont B, et al. Multinational impact of the 1968 Hong Kong influenza pandemic: evidence for a smoldering pandemic. J Infect Dis. 2005;192:233–248. doi:10.1086/431150

[7] Wu J, Ma E, Lee C, et al. The infection attack rate and severity of 2009 pandemic H1N1 influenza in Hong Kong. Clin Infect Dis. 2010;51:1184–1191. doi:10.1086/656740

[8] Kong W, Wang F, Dong B, et al. Novel reassortant influenza viruses between pandemic (H1N1) 2009 and other influenza viruses pose a risk to public health. Microb Pathog. 2015;89:62–72. doi:10.1016/j.micpath.2015.09.002

[9] Smith GJD, Vijaykrishna D, Bahl J, et al. Origins and evolutionary genomics of the 2009 swine-origin H1N1 influenza A epidemic. Nature. 2009;459:1122–1125. doi:10.1038/nature08182

[10] Nelson MI, Vincent AL. Reverse zoonosis of influenza to swine: new perspectives on the human-animal interface. Trends Microbiol. 2015;23:142–153. doi:10.1016/j.tim.2014.12.002

[11] Xiong W, Cowling BJ, Tsang TK. Influenza resurgence after relaxation of public health and social measures, Hong Kong, 2023. Emerg Infect Dis. 2023;29:2556–2559. doi:10.3201/eid2912.230937

[12] Mak GCK, Lau SSY, Wong KKY, et al. Low prevalence of seasonal influenza viruses in Hong Kong, 2022. Influenza Other Respir Viruses. 2023;17:e13123. doi:10.1111/irv.13123

[13] Li X-x, Li C, Du P-c, et al. Rapid and accurate detection of SARS Coronavirus 2 by nanopore amplicon sequencing. Front Microbiol. 2022;13:735363. doi:10.3389/fmicb.2022.735363

[14] Nimsamer P, Sawaswong V, Klomkliew P, et al. "Nano COVID-19": nanopore sequencing of spike gene to identify SARS-CoV-2 variants of concern. Exp Biol Med (Maywood). 2023;248:1841–1849. doi:10.1177/15353702231190931

[15] Zhou B, Donnelly ME, Scholes DT, et al. Single-reaction genomic amplification accelerates sequencing and vaccine production for classical and swine origin human influenza a viruses. J Virol. 2009;83:10309–10313. doi:10.1128/JVI.01109-09

[16] Zhou B, Lin X, Wang W, et al. Universal influenza B virus genomic amplification facilitates sequencing, diagnostics, and reverse genetics. J Clin Microbiol. 2014;52:1330–1337. https://doi.org/10.1128/JCM.03265-13.

[17] De Coster W, Rademakers R. Nanopack2: population-scale evaluation of long-read sequencing data. Bioinformatics. 2023; 39(5):btad311. doi:10.1093/bioinformatics/btad311

[18] Ondov BD, Treangen TJ, Melsted P, et al. Mash: fast genome and metagenome distance estimation using MinHash. Genome Biol. 2016;17:132. doi:10.1186/s13059-016-0997-x

[19] Patrick M. FluStAR: Flu subtyping and assembly resource. 2019; Github. https://github.com/pkmitchell/FluStAR.

[20] Li H. Minimap2: pairwise alignment for nucleotide sequences. Bioinformatics. 2018;34:3094–3100. doi:10.1093/bioinformatics/bty191

[21] Danecek P, Bonfield JK, Liddle J, et al. Twelve years of SAMtools and BCFtools. Gigascience. 2021;10(2):giab008. doi:10.1093/gigascience/giab008

[22] Robinson JT, Thorvaldsdóttir H, Winckler W, et al. Integrative genomics viewer. Nat Biotechnol. 2011;29:24–26. doi:10.1038/nbt.1754

[23] Katoh K, Rozewicki J, Yamada KD. MAFFT online service: multiple sequence alignment, interactive sequence choice and visualization. Brief Bioinform. 2019;20:1160–1166. doi:10.1093/bib/bbx108

[24] Stamatakis A. RAxML version 8: a tool for phylogenetic analysis and post-analysis of large phylogenies. Bioinformatics. 2014;30:1312–1313. doi:10.1093/bioinformatics/btu033

[25] Yang Z. PAML 4: phylogenetic analysis by maximum likelihood. Mol Biol Evol. 2007;24:1586–1591. doi:10.1093/molbev/msm088

[26] Aksamentov I, Roemer C, Hodcroft EB, et al. Nextclade: clade assignment, mutation calling and quality control for viral genomes. The J Open Source Softw. 2021;6(67):3773. doi:10.21105/joss.03773

[27] Galili T. Dendextend: an R package for visualizing, adjusting and comparing trees of hierarchical clustering. Bioinformatics. 2015;31:3718–3720. doi:10.1093/bioinformatics/btv428

[28] Tonkin-Hill G, Lees JA, Bentley SD, et al. An R implementation of the population clustering algorithm hierBAPS. Wellcome Open Res. 2018;3:93. doi:10.12688/wellcomeopenres.14694.1

[29] Cheng L, Connor TR, Siren J, et al. Hierarchical and spatially explicit clustering of DNA sequences with BAPS software. Mol Biol Evol. 2013;30:1224–1228. doi:10.1093/molbev/mst028

[30] Waterhouse A, Bertoni M, Bienert S, et al. SWISS-MODEL: homology modelling of protein structures and complexes. Nucleic Acids Res. 2018;46:W296–W303. doi:10.1093/nar/gky427

[31] Bertoni M, Kiefer F, Biasini M, et al. Modeling protein quaternary structure of homo- and hetero-oligomers beyond binary interactions by homology. Sci Rep. 2017;7:10480. doi:10.1038/s41598-017-09654-8

[32] Boyoglu-Barnum S, Ellis D, Gillespie RA, et al. Quadrivalent influenza nanoparticle vaccines induce broad protection. Nature. 2021;592:623–628. doi:10.1038/s41586-021-03365-x

[33] Lei R, Tan TJC, Hernandez Garcia A, et al. Prevalence and mechanisms of evolutionary contingency in human influenza H3N2 neuraminidase. Nat Commun. 2022;13:6443. doi:10.1038/s41467-022-34060-8

[34] Lin YP, Xiong X, Wharton SA, et al. Evolution of the receptor binding properties of the influenza A(H3N2) hemagglutinin. Proc Natl Acad Sci USA. 2012;109:21474–21479. doi:10.1073/pnas.1218841110

[35] Yang H, Carney PJ, Mishin VP, et al. Molecular characterizations of surface proteins hemagglutinin and neuraminidase from recent H5Nx avian influenza viruses. J Virol. 2016;90:5770–5784. doi:10.1128/jvi.00180-16
[36] Meng EC, Goddard TD, Pettersen EF, et al. UCSF chimerax: tools for structure building and analysis. Protein Sci. 2023;32:e4792. doi:10.1002/pro.4792
[37] Murphy C, Kwan MYW, Chan ELY, et al. Influenza vaccine effectiveness against hospitalizations associated with influenza A(H3N2) in Hong Kong children aged 9 months to 17 years, June-November 2023. Vaccine. 2024;42:1878–1882. doi:10.1016/j.vaccine.2024.02.056
[38] Barr IG, Subbarao K. Implications of the apparent extinction of B/Yamagata-lineage human influenza viruses. npj Vaccines. 2024;9:219. doi:10.1038/s41541-024-01010-y
[39] World Health Organization. Influenza updates archive; 2023.
[40] Achangwa C, Park H, Ryu S, et al. Collateral impact of public health and social measures on respiratory virus activity during the COVID-19 pandemic 2020–2021. Viruses. 2022;14(5):1071. doi:10.3390/v14051071
[41] Tsang TK, Perera RAPM, Fang VJ, et al. Reconstructing antibody dynamics to estimate the risk of influenza virus infection. Nat Commun. 2022;13:1557. doi:10.1038/s41467-022-29310-8
[42] Krammer F. The human antibody response to influenza A virus infection and vaccination. Nat Rev Immunol. 2019;19:383–397. doi:10.1038/s41577-019-0143-6
[43] Krauland MG, Galloway DD, Raviotta JM, et al. Impact of low rates of influenza on next-season influenza infections. Am J Prev Med. 2022;62:503–510. doi:10.1016/j.amepre.2021.11.007
[44] Baker RE, Park SW, Yang W, et al. The impact of COVID-19 nonpharmaceutical interventions on the future dynamics of endemic infections. Proc Natl Acad Sci U S A. 2020;117:30547–30553. doi:10.1073/pnas.2013182117
[45] Yang B, Lin Y, Xiong W, et al. Comparison of control and transmission of COVID-19 across epidemic waves in Hong Kong: an observational study. Lancet Reg Health West Pac. 2024;43:100969. doi:10.1016/j.lanwpc.2023.100969
[46] Chan YD, Wong ML, Au KW, et al. Seasonal influenza vaccine effectiveness at primary care level, Hong Kong SAR, 2017/2018 winter. Hum Vaccin Immunother. 2019;15:97–101. doi:10.1080/21645515.2018.1514222
[47] Chan Y-w, Wong M-l, Kwok F-y, et al. The effect of seasonal influenza vaccine on medically-attended influenza and non-influenza respiratory viruses infections at primary care level, Hong Kong SAR, 2017/18 to 2019/20. Vaccine. 2021;39:3372–3378. doi:10.1016/j.vaccine.2021.04.059
[48] O'Neill GK, Taylor J, Kok J, et al. Circulation of influenza and other respiratory viruses during the COVID-19 pandemic in Australia and New Zealand, 2020–2021. Western Pac Surveill Response J. 2023;14:1–9. doi:10.5365/wpsar.2023,14.3.948
[49] Zhao P, Zhang Y, Wang J, et al. Epidemiology of respiratory pathogens in patients with acute respiratory infections during the COVID-19 pandemic and after easing of COVID-19 restrictions. Microbiol Spectr. 2024;12:e0116124. doi:10.1128/spectrum.01161-24
[50] Cao L, Lou J, Zhao S, et al. In silico prediction of influenza vaccine effectiveness by sequence analysis. Vaccine. 2021;39:1030–1034. doi:10.1016/j.vaccine.2021.01.006
[51] Wang MH, Lou J, Cao L, et al. Characterization of key amino acid substitutions and dynamics of the influenza virus H3N2 hemagglutinin. J Infect. 2021;83:671–677. doi:10.1016/j.jinf.2021.09.026
[52] Liu Y, Jin W, Guan W, et al. The genetic characterization of hemagglutinin (HA), neuraminidase (NA) and polymerase acidic (PA) genes of H3N2 influenza viruses circulated in Guangdong Province of China during 2019-2020. Virus Genes. 2022;58:392–402. doi:10.1007/s11262-022-01923-7